ROBUST STRUCTURAL DESIGN FOR ACTIVE AEROELASTIC WING WITH AERODYNAMIC UNCERTAINTIES

P. Scott Zink[*], Daniella E. Raveh[†], Dimitri N. Mavris[‡]
Aerospace Systems Design Laboratory
School of Aerospace Engineering
Georgia Institute of Technology, Atlanta, Georgia, 30332-0150

Abstract

A multidisciplinary design study for Active Aeroelastic Wing technology considering the uncertainty in maneuver loads estimated by linear aerodynamic theory is presented. The study makes use of a design of experiments/response surface methodology and modal-based structural optimization to construct deterministic relationships between wing structural weight and control laws design, based on linear aerodynamics. CFD Navier-Stokes analysis is then used to define typical differences between rigid aerodynamic loads as predicted by nonlinear and linear theory. These differences are then used to define aerodynamic uncertainties in a probabilistic manner, which are propagated, through Latin Hypercube Sampling and modal-based static aeroelastic analysis, to a response function that represents the magnitude of structural redesign. Structural designs then are sought that are both low weight and whose performance is relatively invariant in the presence of load uncertainty. The motivation for this study is derived by the frequent inability to accurately represent maneuver loads on an aircraft structure, which often requires redesign (sometimes major) late in the design process as loads predictions become more accurate.

Introduction

The structural design process of airframe companies is generally an iterative process between control laws design, load analysis, and structural analysis/design. In this process, the airframe is laid out and sized to meet various objectives, such as producibility, affordability, fit and function, and structural integrity across the entire flight envelope[1]. In particular, for agile fighter aircraft, the maneuver flight loads, which are a subset of all the loads that are analyzed, play a key part in the design of the structure as a large portion of the airframe is sized by these loads to meet strength, static

---

aeroelastic effectiveness, and dynamic aeroelastic requirements[2]. Maneuver loads refer to those aerodynamic and inertial loads produced by a wide array of maneuvers which include symmetric maneuvers, asymmetric maneuvers, evasive maneuvers, deep and flat spins, and gusts[3]. These loads naturally depend heavily on aerodynamics, weights, structures and flight control laws[4], hence the iterative nature of the structural design process. Over the course of this iterative process, the maneuver loads are continuously refined to include more complex and accurate models, from empirical estimations or linear aerodynamics in the initial phases to Computational Fluid Dynamics (CFD) models, wind tunnel testing, and finite element aeroelastic effects in the latter stages of design[5]. As the structural design depends heavily on the loads, it too is refined as the loads models improve[1].

This sequential, iterative structural design process is often expensive, as the structure is continually being designed and redesigned usually with ever increasing weight. It often reveals the need for major design modifications (to both the structure and control laws) late in the design process, if load characteristics to which the structure was designed are not accurately predicted. For example, structural load characteristics of the X-29A associated with center of gravity position, the backup flight control system, and buffet were not fully predicted before flight test leading to modification of the control laws[6]. In another case, leading edge loads of the recently developed Eurofighter 2000 at transonic Mach numbers turned out to be higher than anticipated[5]. During the design of the F-16, the design and analysis assumptions were unable to cover all load scenarios, offering some "surprises in terms of external loads acting on the aircraft" and resulting, in one instance, in a fleet wide retrofit of an element of the upper wing skin structure[7]. As indicated by a few "real life" examples, the inability to accurately represent loads on an aircraft structure comes at the price of increased weight, longer design cycle times, and/or compromised performance. As a result, there is a motivation to acquire structural designs, at the earliest phases of the design process, that are robust to inaccurate loads, without imposing an unacceptable degree of conservatism. In doing so, the iterations between loads estimations and structural design may be

reduced, thus shortening design cycle time, and reducing the chances of major structural redesign late in the aircraft's development. In this context, a robust structural design is defined to be one that is low weight and has low variation due to uncertainty in maneuver loads.

Existing structural design methods are strained even further when new technologies are to be examined. Active aeroelastic wing (AAW) technology[8], currently in a flight test research program at the Air Force[9], provides some unique challenges to the structural design of future fighter aircraft. AAW technology makes use of redundant wing control surfaces to provide maneuver load control and increased roll authority. AAW design is inherently multidisciplinary, combining aerodynamics, active controls, and structures, to provide a net benefit to aircraft performance. It exploits the use of leading and trailing edge control surfaces to aeroelastically shape the wing, with the resulting aerodynamic forces from the flexible wing becoming the primary means for generating control power. With AAW, the control surfaces then act mainly as tabs and not as the primary sources of control power as they do with a conventional control approach. As a result, wing flexibility is seen as an advantage rather than a detriment, since the aircraft can be operated beyond control surface reversal speeds and still generate the required control power for maneuvers. The differences between AAW technology and a conventional control approach are illustrated conceptually in Figure 1. The hypothetical example shows the cross section of two wings deforming due to aeroelastic effects, where the AAW on the left is twisting in a positive way with the use of both leading and trailing edge surfaces, and the conventionally controlled wing on the right, using only the trailing edge surface, is twisting in a negative way.
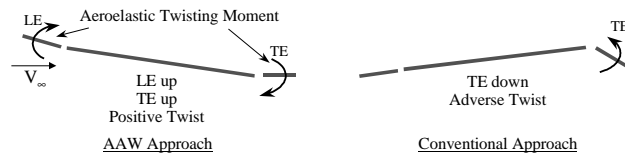

Figure 1 – Illustration of AAW Technology

The AAW design process refers to the concurrent optimization of the structural elements and the control surface deflections or *gear ratios*. The control surface gear ratios dictate how one control surface deflects with respect to a single independent surface. Two gear ratio scenarios are illustrated in Figure 2 in which the deflections of the leading edge inboard (LEI), leading edge outboard (LEO), and trailing edge inboard (TEI) surfaces are linearly dependent on the deflection of the trailing edge outboard surface (TEO). Historically,

design of the gear ratios, more commonly known as trim optimization, has comprised of a direct gradient-based optimization formulation. By this approach, the gear ratios are optimized to minimize an objective of stress, component loads and/or control power[10,11,12,13,14]. The typical approach to the AAW design process then involves embedding trim optimization in an iterative process with structural optimization, to arrive at a simultaneous optimal control law and structural gauges. Reference [14] presents such an AAW design process in detail.
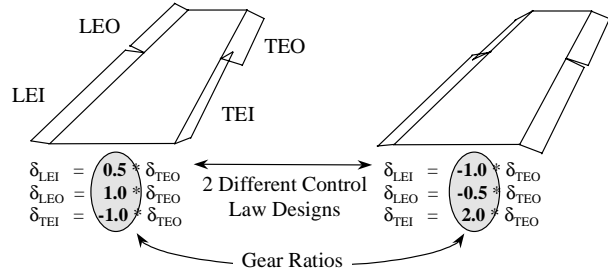

Figure 2 – Gear Ratio Illustration

In contrast to the typical AAW design processes, Reference [15] approached the AAW design process in a probabilistic manner, seeking designs that were robust to small changes in the gear ratios. Changes in the gear ratios occur often over the course of the design process when the control laws are evolving. In Reference [15], a design of experiments/ response surface methodology (DOE/RSM)[16,17] was employed, in which a response surface equation (RSE) of structural wing weight versus the gear ratios was generated. Recently developed tools for modal based structural optimization[18,19] provided efficient and accurate estimation of wing weight. Using the RSE, one could then find the set of gear ratios that produced the lowest weight structure. However, the aim of the study was not only to find low weight structural designs, but also robust structural designs (i.e., designs that were low weight but that required little redesign for small changes in the gear ratios). The control surface gear ratios were then assigned probability density functions (PDF) in order to model the changes in gear ratios that typically occur over the design process. Using the advanced mean value (AMV)[20,21] method, cumulative distribution functions (CDF) of a response, which reflected the magnitude of redesign, were generated for each structural design used in obtaining the weight RSE. This response function was calculated by finite element analysis of the structural design, evaluating the strain constraints, and then summing them, with additional penalties for violated constraints. A *robustness metric* was assigned to each of the structural designs, giving the structural designer additional information, typically not available

in traditional design processes, with which to make design decisions.

The current research expands upon the work of Reference [15] by examining uncertainties in the maneuver loads. AAW design methods rely on linear aerodynamic theory for estimation of maneuver loads. Depending on the flight regime of interest, there may be significant discrepancies between the predicted loads and actual loads. As a result, there is significant uncertainty associated with maneuver loads estimated by linear aerodynamics. This uncertainty could be alleviated by the use of recently developed tools for CFD-based maneuver loads analysis and structural optimization schemes[22,23], in which the structural optimization is based on trimmed maneuver loads evaluated by a CFD analysis. However, in consideration of a preliminary design study, in which multiple load evaluations are needed, extensive use of CFD codes may be impractical. Thus, the retention of computationally inexpensive linear aerodynamic methods is desirable, as long as the structural design methodology accounts for the inherent uncertainty associated with their use, and provides ways to mitigate its effect. The present study presents a probabilistic methodology to evaluate the effect of uncertainties in the aerodynamic load evaluation on the structural design. DOE/RSM techniques are first used to construct the relationship between wing structural weight and gear ratios, based on linear aerodynamics. Then, a CFD Navier-Stokes analysis of the loads acting on the rigid configuration is used to define typical differences between linear and nonlinear wing loading. These differences are used to define the *aerodynamic uncertainties* in a probabilistic manner. Then, for each structural design, these uncertainties are propagated to responses of interest to the structural designer. The probabilistic characteristics of the response parameters can be used to evaluate the robustness of these designs, and allow for a trade-off study between weight, performance and robustness to be performed. The probabilistic information can be used to define the best overall design, and also to identify the design conditions for which early accurate evaluation of the aerodynamic loads is most important.

Mathematical Models

Design of Experiments/Response Surface Methodology

The DOE/RSM techniques used to construct the relationship between wing weight and the gear ratios employ intelligent design of experiments and statistical multivariate regression to relate a response to a set of contributing variables[17]. Many times the relationship between the response and the design variables is either too complex or unknown, so that it becomes necessary to use an empirical approach to build an approximate

model of the exact relationship. The model, for the purposes of this study, is a 2nd order equation, also referred to as a response surface equation (RSE), which takes the following form:

$$R = b_0 + \sum_{i=1}^{k} b_i x_i + \sum_{i=1}^{k} b_{ii} x_i^2 + \sum_{i=1}^{k-1} \sum_{j=i+1}^{k} b_{ij} x_i x_j \quad (1)$$

where b_i are coefficients for the first degree terms, b_{ii} are coefficients for the pure quadratic terms, b_{ij} are the coefficients for the cross-product terms, x_i are the design variables which, in the case of this study, are the gear ratios, and R is the response, most notably structural wing weight, being approximated. These coefficients are estimated using least squares regression of experimental or computer simulated data, which is provided in an organized manner through a design of experiments[17].

After checking the statistical and predictive accuracy of the RSE within the designated design space, the designer can use the RSE as a convenient model with which to examine a very complex design space. For a given point in the gear ratio design space, the weight can be estimated by the quadratic Equation (1), avoiding expensive finite element analysis and optimization.

Introduction of Aerodynamic Uncertainty to the Aeroelastic Equations

The basic equation for the static aeroelastic analysis of a free aircraft by the finite element method in discrete coordinates is[25]:

$$[[K] - q[AICS]]\{u\} + [M][\phi_r]\{\ddot{u}_r\} = [P]\{\delta\} \quad (2)$$

where $[K]$ is the stiffness matrix, $[AICS]$ is the aerodynamic influence coefficients matrix transformed to the structural degrees of freedom, $\{u\}$ are the displacements and rotations at the structural nodes, $[M]$ is the mass matrix, $[\phi_r]$ are the rigid body modes of the free aircraft, $\{\ddot{u}_r\}$ is a vector of rigid body accelerations, $[P]$ is a matrix of the rigid aerodynamic force coefficients due to aerodynamic trim parameters, q is the dynamic pressure, and $\{\delta\}$ is the aerodynamic trim parameter values (e.g., angle of attack, aileron deflection, pitch rate). The matrix $[P]$ contains columns corresponding to the rigid aerodynamic forces due to a unit deflection of each of the trim parameters, plus a column for each of the control surfaces. A typical $[P]$ matrix for a symmetric maneuver of the AAW model would look like:

$$[P] = [\{P\}_{LEI}, \ \{P\}_{LEO}, \ .... \ \{P\}_\alpha, \{P\}_{Prate}] \ (3)$$

The aerodynamic load vectors are normally estimated by linear aerodynamic panel codes, in the aerodynamic grid points, and then transformed to the structural grids through a spline matrix. It is these

vectors that the authors are suggesting to augment with uncertainty models.

Uncertainty in the rigid aerodynamic force coefficients ($\{P\}_i$) is introduced to the static aeroelastic equation through the following formulation:

$$\{P\}_i = \{P\}_i^{linear} + \eta_i\{\Delta P\}_i \qquad (4)$$

where i refers to the aerodynamic trim parameter of interest, $\{P\}^{linear}$ is the vector of rigid aerodynamic force coefficients as predicted by linear aerodynamic theory, and $\{\Delta P\}_i$, herein referred to as a "noise mode," is defined as:

$$\{\Delta P\}_i = \{P\}_i^{nonlinear} - \{P\}_i^{linear} \qquad (5)$$

The vector $\{P\}^{nonlinear}$ refers to the rigid aerodynamic forces due to a unit deflection of the trim parameter, as computed by a CFD analysis or provided by wind tunnel test. Since the purpose of introducing the noise mode is to capture nonlinear aerodynamic characteristics, which are not always evident at an angle of attack of one degree, $\{P\}^{nonlinear}$ is evaluated for a larger angle of attack and then normalized by the angle of attack used to compute it. This implies that the role of $\{P\}^{nonlinear}$ is not to introduce accurate load estimation into the aeroelastic analysis, but rather to introduce a measure of how the nonlinear load distribution may vary from the linear. The significance of the contribution of $\{\Delta P\}_i$ to the total force coefficient vector is related through a random variable, η_i. The PDF associated with η_i takes on values from 0 to 1, where 0 corresponds to purely linear rigid loads and 1 corresponds to purely nonlinear rigid loads.

As redundant control surfaces are being used to trim the aircraft, a gearing matrix, $[G]$, is introduced to the right hand side (RHS) of Equation (2) which relates the deflection of the dependent surfaces, $\{\delta\}$, to the independent surface(s), $\{\delta_l\}$, so that the RHS becomes:

$$RHS = [P][G]\{\delta_1\} \qquad (6)$$

With the introduction of the load uncertainty model, and some rearrangement of terms, Equation (7) becomes:

$$RHS = [P]^{linear}[G]\{\delta_1\} + [P]^{noise}[G]\{\delta_1\} \qquad (8)$$

where:

$$[P]^{noise} = [\eta_{LEI}\{\Delta P\}_{LEI}, \ \eta_{LEO}\{\Delta P\}_{LEO}, \ .... \ \eta_\alpha\{\Delta P\}_\alpha] \qquad (9)$$

For a free aircraft, Equation (2) is then solved together with the following constraint on the elastic displacements which is based on the assumption that the structural displacements, $\{u\}$, do not change the location and orientation of the center of mass[24]:

$$[\phi_r]^T[M]\{u\} = \{0\} \qquad (10)$$

Equation (2) is used to define $\{u\}$ as a function of $\{\delta\}$, which involves the numerically-heavy decomposition of ($[K]-q[AICS]$). Substitution of $\{u\}$ from Equation (2) into Equation (10) yields the trim equation[25]:

$$[L]\{\ddot{u}_r\} = [R]\{\delta_1\} \qquad (11)$$

where $[L]$ is the resultant aeroelastic mass, and $[R]$ is the resultant aeroelastic trim forces matrix.

As modal-based analysis and optimization is being employed, the discrete displacements, $\{u\}$, of Equation (2) are represented by a linear combination of the modes of vibration as given by:

$$\{u\} = [\phi_r \quad \phi_e]\begin{Bmatrix} \xi_r \\ \xi_e \end{Bmatrix} \qquad (12)$$

where $[\phi_r \quad \phi_e]$ is the modal matrix comprised of the rigid body modes, $[\phi_r]$, of the free aircraft and a subset of the elastic modes, $[\phi_e]$, $\{\xi_r\}$ are the rigid body displacements, and $\{\xi_e\}$ are the elastic modal displacements. Then, pre-multiplication of Equation 2 (with the new formulation for the RHS) by the transpose of the modal matrix, results in the RHS becoming:

$$RHS^{modal} = [\phi_r \quad \phi_e]^T\left([P]^{linear}[G]\{\delta_1\} + [P]^{noise}[G]\{\delta_1\}\right) \qquad (13)$$

or in simplified notation:

$$RHS^{modal} = [GPA]^{linear}\{\delta_1\} + [GPA]^{noise}\{\delta_1\} \qquad (14)$$

As a result of introducing uncertainty to only the right hand side of the static aeroelastic equation, the CPU-intensive decomposition of the left hand side does not have to be performed every time the noise variables change. This is especially beneficial, as probabilistic methods, particularly sampling methods, require many function evaluations to generate a CDF of a system response. This allows for application of more accurate probabilistic methods, such as the Latin Hypercube Sampling (LHS)[26].

Numerical Example

Figure 3 shows the structural model used both in Reference [15] and the current study. It is a preliminary-design finite-element model of a lightweight fighter composite aircraft with 4 wing control surfaces (2 trailing edge, 2 leading edge) and a horizontal tail[18]. The skins of the wing are made up of 4 composite orientations, 0°, ±45°, and 90° plies, where the thickness of the -45° and +45° orientations are constrained to be equal. The composite wing skin plies are designed in thickness, via the structural optimization tool, ASTROS[27,28].
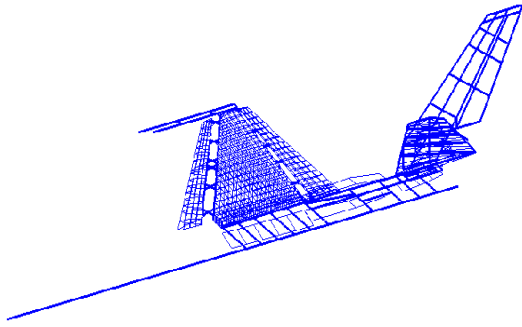
Figure 3 - Structural Model

The linear aerodynamic model, from which the linear force coefficients $\{P\}^{linear}$ are estimated, is shown in Figure 4. It is a flat panel Carmichael[29] model containing 143 vertical panels and 262 horizontal panels. ASTROS has been modified to allow inclusion of Carmichael panel geometry and aerodynamic influence coefficients which then replace the existing aerodynamic database entities created by USSAERO, ASTROS' original aerodynamics module[27].
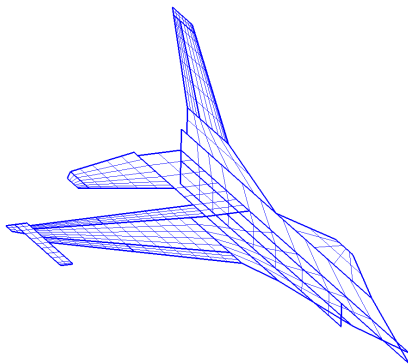

Figure 4 - Linear Aerodynamic Model

The wing section of the nonlinear aerodynamic model is shown in Figure 5. The flow-field around the wing and fuselage was evaluated using an H-type grid, with 4 grid zones representing the upper and lower wing and its wake, and the upper and lower fuselage and its wake. Grid dimensions are 165x41x31 for the wing zones and 165x13x31 for the fuselage zones. The wing itself is represented by 62 grid points in the chordwise direction, 25 grid points in the spanwise direction, and 31 grid points in a direction perpendicular to the wing surface. The flow is analyzed by the CFL3D[30] Euler/Navier-Stokes code. Figure 6 shows pressure coefficient contours on the upper wing surface at a Mach number of 0.9 and 6 degrees angle of attack, which is typical for the maneuvers that this fighter performs. The flow field shown in Figure 6 is the result of a Navier-Stokes analysis, implementing the

Spalart-Allmaras turbulent model. At the outer part of the span the flow was found to be separated at the leading edge, which is typical of very thin airfoils as the one in this case study which has a 4% thickness-to-chord ratio profile. The nonlinear forces acting on the wing surface at this flight condition were normalized by the angle of attack and splined to the wing's structural grids using the spline technique of Reference [31]. These loads then served as $\{P\}_{\alpha}^{nonlinear}$ in Equation (5), and were used to predict the loading uncertainties due to a unit angle of attack. For the nonlinear force vector due to a unit deflection of a control surface, the flow analysis was repeated for the same flight condition, with the elevator deflected to one degree. The loads corresponding to the analysis without surface deflection were subtracted from loads corresponding to the analysis with the surface deflection to provide the net nonlinear load distribution due to the surface deflection.
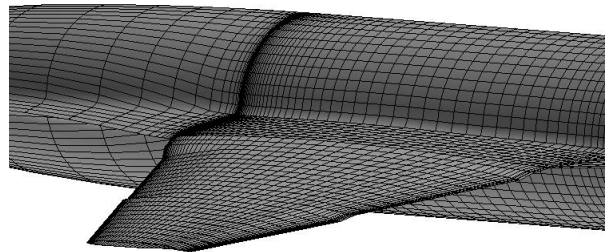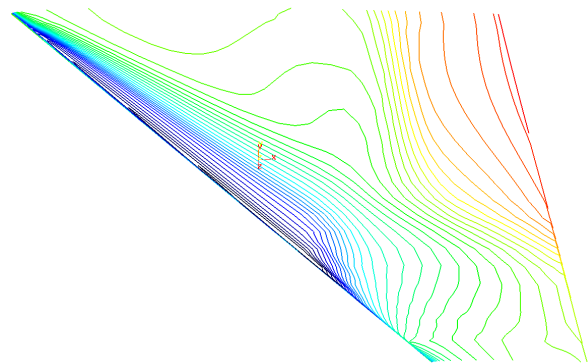

Figure 5 - Nonlinear Aerodynamic Model

Figure 6 - Pressure Coefficient Contours on Wing
Upper Surface (Mach 0.9, $\alpha = 6°$)

The design variables for the structural optimization are the layer thickness of the composite skins. The number of design variables is 78 due to physical linking of the skin elements. Internal structure and carry-thru structure are fixed. Table 1 presents the maneuver conditions and strength constraints to which the structure is designed.

Table 1 - Maneuver Conditions and Design Constraints

Maneuver Condition	Design Constraint
1) Mach 0.95, 10,000 ft. 9g Pull Up	fiber strain: 3000 με tension 2800 με compression
2) Mach 1.20, Sea Level -3g Push Over	fiber strain: 3000 με tension 2800 με compression
3) Mach 1.20, Sea Level Steady State Roll = $100^O/s$	fiber strain: 1000 με tension 900 με compression
4) Mach 0.95, 10,000 ft. Steady State Roll = $180^O/s$	fiber strain: 1000 με tension 900 με compression

Table 2 – Gear Ratio Design Variables and Ranges

Design Variable	Corresponding Surface	Maneuver	Min.	Max.
XLEI1	L.E. Inboard	Subsonic Pull-Up	-1.0	0.4
XLEO1	L.E. Outboard	Subsonic Pull-Up	-1.0	0.4
XTEI1	T.E. Inboard	Subsonic Pull-Up	-1.0	1.0
XTEO1	T.E. Outboard	Subsonic Pull-Up	-1.0	1.0
XLEI2	L.E. Inboard	Super. Push-Over	-1.0	0.4
XLEO2	L.E. Outboard	Super. Push-Over	-1.0	0.4
XTEI2	T.E. Inboard	Super. Push-Over	-1.0	1.0
XTEO2	T.E. Outboard	Super. Push-Over	-1.0	1.0
XTAIL3	Horiz. Tail	Supersonic Roll	-0.065	2.0
XLEI3	L.E. Inboard	Supersonic Roll	-0.16	2.0
XTEI3	T.E. Inboard	Supersonic Roll	-2.0	0.16
XTEO3	T.E. Outboard	Supersonic Roll	-2.0	0.16
XTAIL4	Horiz. Tail	Subsonic Roll	-0.08	1.0
XLEI4	L.E. Inboard	Subsonic Roll	-0.22	0.4
XLEO4	L.E. Outboard	Subsonic Roll	-0.22	0.5
XTEI4	T.E. Inboard	Subsonic Roll	-0.22	2.0

Table 3 – Responses and Notation

Response	Notation	Unit
Designed Structural Wing Weight	Weight	lb
Hinge Moment LEI – Maneuver 1	HM_LEI1	lb-in
Hinge Moment LEO – Maneuver 1	HM_LEO1	lb-in
Hinge Moment TEI – Maneuver 1	HM_TEI1	lb-in
Hinge Moment TEO – Maneuver 1	HM_TEO1	lb-in
Hinge Moment LEI – Maneuver 2	HM_LEI2	lb-in
Hinge Moment LEO – Maneuver 2	HM_LEO2	lb-in
Hinge Moment TEI – Maneuver 2	HM_TEI2	lb-in
Hinge Moment TEO – Maneuver 2	HM_TEO2	lb-in
Hinge Moment LEI – Maneuver 3	HM_LEI3	lb-in
Hinge Moment LEO – Maneuver 3	HM_LEO3	lb-in
Hinge Moment TEI – Maneuver 3	HM_TEI3	lb-in
Hinge Moment TEO – Maneuver 3	HM_TEO3	lb-in
Hinge Moment LEI – Maneuver 4	HM_LEI4	lb-in
Hinge Moment LEO- Maneuver 4	HM_LEO4	lb-in
Hinge Moment TEI – Maneuver 4	HM_TEI4	lb-in
Hinge Moment TEO – Maneuver 4	HM_TEO4	lb-in

For each maneuver, the deflections of 4 of the 5 control surfaces are linked to the remaining surface (known as *basis surface*) via the gear ratios defined in the CONLINK bulk data card. This basis surface then is the free variable in the ASTROS trim module and the deflections of all the other surfaces are dependent upon it.

The horizontal tail was selected as the basis surface for Maneuvers 1 & 2, since it has historically been the primary control surface for symmetric trim. The LEO surface was selected for Maneuver 3, because it is the most effective surface at supersonic conditions. Both trailing edge surfaces experience control reversal at supersonic flight, thus quickly ruling them out as candidates for the basis surface of Maneuver 3. For Maneuver 4, the TEO surface was chosen, since it is the most effective roll control surface at subsonic speeds.

Robust Aeroelastic Wing Design Method

Design Space Definition

The first phase of the methodology is to understand how the structural designs are characterized by the gear ratios. This requires building relationships between structural responses, such as designed structural weight and hinge moments, and the gear ratios.

The gear ratios that this study is examining, and the ranges of each, are defined in Table 2. Since there are four maneuvers to which the structure is sized, and four gear ratios per maneuver, there are a total of 16 gear ratios that are of interest. The range of each gear ratio was established in part by the maximum and minimum deflection of the control surface to which it corresponds. The responses of interest are listed in Table 3, as well as their notation that will be used throughout the remainder of the paper.

Of all the responses, the structural weight is the most important because it does the best job of capturing the overall "goodness" of the structural design. The hinge moments are important, because they directly affect actuator weight and required power. Given a fixed actuator with maximum allowable moment, the hinge moment responses can be considered as constraints in the design space.

Screening Test

The relationships between structural characteristics and gear ratios are approximated by RSEs using DOE/RSM techniques. However, the 16 design variables (gear ratios) delineated in Table 2 envelop a sizeable design space. Thus, it is desirable to screen out some variables to reduce the size of the problem to a manageable level, while at the same time

acknowledging that many of the variables will be relatively insignificant.

The screening test is a 128-case, 2-level fractional factorial DOE, meaning that each gear ratio is tested only at its minimum and maximum value. The DOE is built using the statistical software JMP[32], and a sample of the screening test is shown in Table 4 where the +1 refers to the maximum value of the gear ratio and -1, to its minimum value. Each row of the DOE corresponds to an "experiment", where each "experiment" is a modal-based structural optimization in ASTROS with different gear ratio values. As a result, each row also corresponds to a different structural design where laminate thickness and percent layer thickness of the structure are different from case to case.

Table 4 – Sample of Screening Test

Case	XLEI1	XLEO1	⋯	XLEO4	XTEI4	Weight (lb)
1	-1	-1	⋯	1	-1	319.7
2	-1	-1	⋯	1	1	312.7
3	-1	-1	⋯	-1	-1	344.0
4	-1	-1	⋯	-1	1	308.4
5	-1	-1	⋯	1	1	303.2
.	.	.	.	.	.	.
.	.	.	.	.	.	.
124	1	1	⋯	1	-1	300.1
125	1	1	⋯	-1	-1	292.1
126	1	1	⋯	-1	1	347.3
127	1	1	⋯	1	-1	342.5
128	1	1	⋯	1	1	285.8

An *effect-screening* is then performed on the extracted data to determine which variables contribute most to wing weight. For this case, the effect-screening involves a linear regression of the weight using only main-effect terms (e.g., XLEI1) and 2nd order interaction terms (e.g., XLEI1*XLEO1). The regression coefficients of each of these terms is then scaled and ranked in order of their influence on wing weight[32]. The 8 most significant gear ratios from the screening test are shown in Table 5. The other 8 gear ratios, that were not particularly significant, were then set to their midpoint values and remained fixed for the remainder of the study.

Table 5 – Surviving Gear Ratios from Screening Test

XLEO1
XTEI1
XTEO1
XTAIL3
XLEI3
XTAIL4
XLEO4
XTEI4

Response Surface Equation

With the size of the problem now reduced, the next step is to build RSEs of the responses of interest as a function of the 8 surviving gear ratios. Creation of the RSEs is similar to that of the screening test in that a DOE is created, responses of interest are calculated for each case and inserted into the appropriate columns, and a regression analysis is performed on the data. The difference, however, is that the screening model is linear, whereas for the RSE it is quadratic. As a result, the DOE must test the design variables not at two levels, as in the screening test, but at three or more levels, to capture quadratic effects.

A 145-case DOE for 8 design variables was chosen for RSE generation. A sample of the DOE is shown in Table 6 where the -1's and +1's correspond to the minimum and maximum values of the gear ratios, respectively, and 0 is the midpoint of the gear ratio within its range.

As previously mentioned, each of the rows of the DOE table refers to a modal-based structural optimization with a different set of gear ratio values for every case. However, unlike the screening test, wing weight is not the only response that is extracted. In addition to weight, the other responses of interest (hinge moments) are extracted and inserted into response columns. Table 6 shows some of the responses for which RSEs are constructed.

For each of the responses, a least squares regression is performed on the data, and RSEs are generated. A few of the more important of these RSEs are displayed in Figure 7. This plot is known as a *prediction profile*, and it provides the designer with a convenient means to gain visibility of the design space as modeled by the RSEs. As the designer changes the values of the gear ratios, he can immediately see the influence of the decision on the responses.

The RSE fit is tested through a validation test, in which the response is evaluated at a number of random points throughout the design space and compared to its value as predicted by the RSE. For this study, the percent difference between the actual weight and the RSE predicted weight rarely exceeded 5%. This indicates that the weight RSE is a reasonably good predictor of the exact relationship.

Table 6 – Sample of RSE DOE

Case	XLEO1	XTEI1	XTEO1	...	XLEO4	XTEI4	Weight	HM_TEO4
1	-1	-1	-1	...	-1	-1	359.4	-29519.0
2	-1	-1	-1	...	1	1	324.0	-12483.5
3	-1	-1	-1	...	-1	1	319.4	-9904.2
4	-1	-1	-1	...	1	-1	320.9	-12802.9
.	.	.	.	.	.	.	.	.
.	.	.	.	.	.	.	.	.
142	0	0	0	...	1	0	295.4	-13057.0
143	0	0	0	...	0	-1	310.8	-18700.6
144	0	0	0	...	0	1	295.5	-11428.1
145	0	0	0	...	0	0	298.2	-13928.1
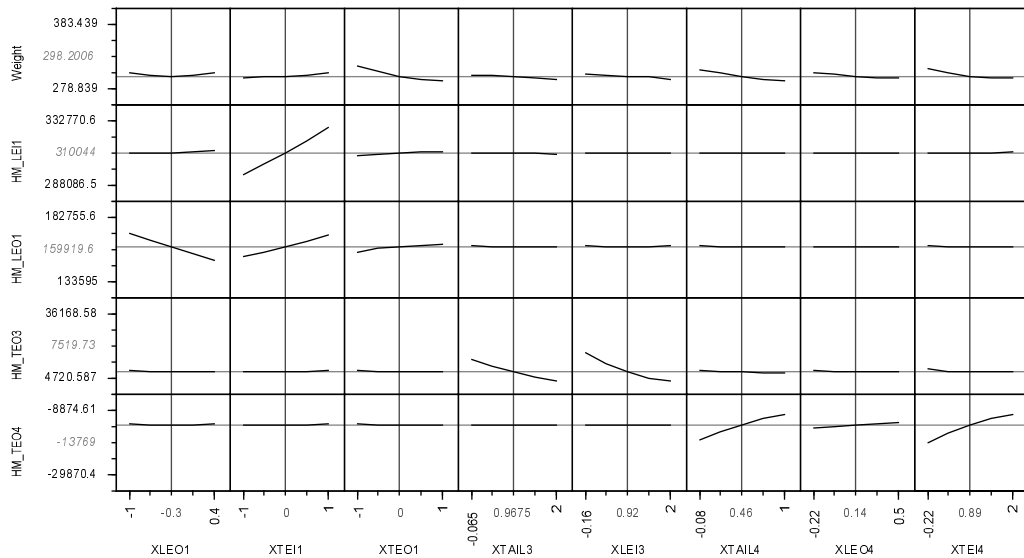
Figure 7 – Sensitivities of Responses to Gear Ratios

With the RSEs determined and validated, the designer could select the gear ratio values that produced the lowest weight, subject to hinge moment constraints. However, this is a deterministic solution and the structural design that results from this selection in gear ratios could perform poorly if the aerodynamic loads differ from their values as predicted by linear aerodynamic theory. As a result, the next step is to evaluate each structural design resulting from each case in the DOE on its ability to meet strength requirements given that the aerodynamic loads associated with the angle of attack and with the control surfaces are uncertain.

Probabilistic Analysis

Noise modes for angle of attack ($\{\Delta P\}_\alpha$) and the TEO surface ($\{\Delta P\}_{TEO}$) have been generated for the subsonic, symmetric maneuver condition. These noise modes correspond to the unit rigid force differences, at the structural degrees of freedom, between nonlinear and linear aerodynamics. To give an indication of the shape of these noise modes, Figures 8, 9, 10, and 11 display chordwise pressure coefficient distributions as predicted by nonlinear and linear aerodynamics for a unit angle of attack and a unit deflection of the TEO surface.

Figure 8 shows the ΔC_p distribution for a unit angle of attack at a semispan of 32%. At this section a shock exists at about 75% of the chord, which the linear aerodynamic theory could not predict. Figure 9 presents the ΔC_p distribution at 92% of the wing semispan, where the flow was found to be separated. At this section, too, the nonlinear ΔC_p is significantly different than the linear. The nonlinear flow analysis predicted greater total lift per unit angle of attack, which resulted in less angle of attack required to trim the aircraft and consequently less aerodynamic loading.

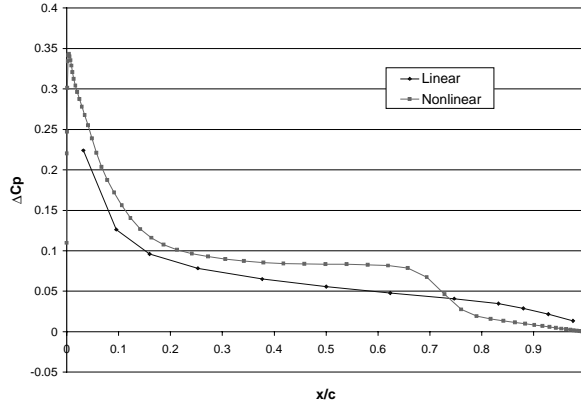American Institute of Aeronautics and Astronautics

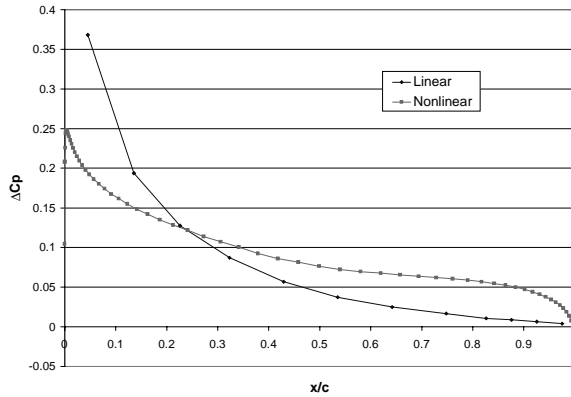Figure 8 - Chordwise ΔC_p Distribution for Unit Angle of Attack (32% Semispan)

Figure 9 - Chordwise ΔC_p Distribution for Unit Angle of Attack (92% Semispan)

Figure 10 is the chordwise ΔC_p distribution for a unit deflection of the TEO surface at a semispan station of 81%. At the TEO hingeline (which occurs at about 80% chord) linear aerodynamic theory predicts a much larger ΔC_p than does nonlinear aerodynamics.
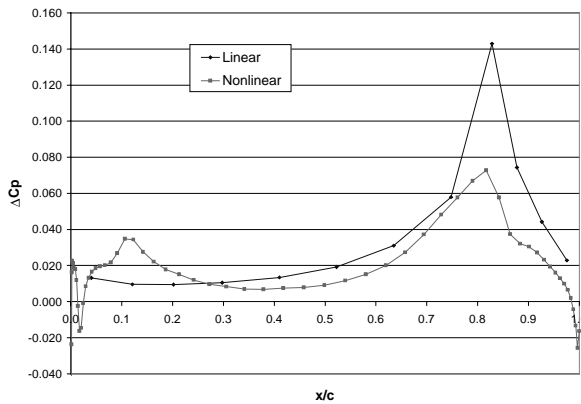

Figure 10 - Chordwise ΔC_p Distribution for Unit Deflection of TEO (81% Semispan)

Similarly, Figure 11 is the chordwise ΔC_p distribution for a unit deflection of the TEO surface at a semispan station of 92%. Once again, linear aerodynamics result in higher load at the trailing edge.
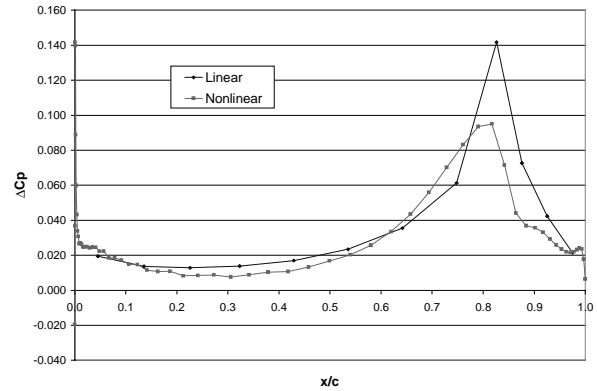

Figure 11 - Chordwise ΔC_p Distribution for Unit Deflection of TEO (92% Semispan)

Since it is desired that each structural design be analyzed on its ability to be invariant to uncertainties in the aerodynamic loads associated with control surfaces and angle of attack, a function is developed that captures the *magnitude of redesign*. For given values of the random noise mode coefficients (η_{LEO}, η_{TEI}, η_{α}, etc.), modal-based static aeroelastic analysis of a structural design is performed, and the resulting strain constraints (used in the previous structural optimization) are calculated. The function that captures the magnitude of redesign then is the summation of all violated constraints that result from this static aeroelastic analysis case, as given by the following equation:

$$F = \sum_{i=1}^{N} g_i \cdot I\left(g_i \geq 0\right) \qquad I = \begin{cases} 1 & g_i \geq 0 \\ 0 & otherwise \end{cases} \qquad (15)$$

$$g_i = \frac{\varepsilon_i}{\varepsilon_{allowable}} - 1.0 \qquad (16)$$

where ε_i are the strain values, $\varepsilon_{allowable}$ are the allowable strain levels, and N is the total number of strain constraints used in the structural optimization.

The function is built on the assumption that those structural designs that have highly violated strain constraints will require larger amounts of redesign than those with smaller amounts of or no violated constraints. One improvement, though, to this function could be to also include the area of the element corresponding to each strain constraint, so that large elements that have violated constraints are penalized more heavily than small elements that have violated constraints.

Probabilistic analysis, to compute a CDF of the redesign function, has been conducted. This probabilistic analysis was performed only for the first structural design of the DOE table and the subsonic, symmetric maneuver with uncertainty associated with the TEO surface. The probabilistic analysis method employed was LHS, which, as previously discussed, has some of the benefits of sampling based methods without the extreme computational expense normally associated with traditional Monte Carlo analyses. A uniform PDF varying from 0 to 1 was assigned to η_{TEO} in an attempt to cover a large range of possible load conditions. One hundred samples of the random variable were generated, and for each random sample, the redesign function was evaluated. Figure 12 is the CDF of the redesign function due to uncertainty in the noise mode coefficient for the TEO surface. What this CDF suggests, based on the fact that there is a 0% chance of the response function being less than zero, is that any noise mode coefficient with a value greater than zero results in a violation of some of the strain constraints. Clearly then, designing the structure (for this particular value of gear ratios) with linear control surface aerodynamics, results in an inadequate solution when subjected to more realistic loads. In addition, the linear nature of the CDF suggests a nearly linear relationship between the redesign function and η_{TEO}.
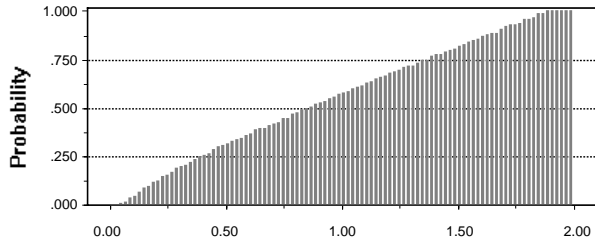

Figure 12 - CDF of Redesign Function

Similar to the TEO outboard surface, a uniform PDF with a range from 0 to 1 was applied to the noise mode coefficient corresponding to angle of attack (η_α). For 100 random samples of η_α, generated by LHS, the redesign function was evaluated and a CDF generated. However, the results of this analysis revealed that all samples resulted in no violated constraints, so that there was a 100% probability of the redesign function being less than zero. This suggests, that for the case studied, the use of linear aerodynamics for the estimation of loads due to angle of attack is conservative, just the opposite of what occurs for the TEO surface. This agrees with the trend found in Reference [31] in which the structure optimized for the nonlinear loads for a 3g pull-up was found to be lighter than a structure optimized for the linear loads. This also suggests that the uncertainty due to angle of attack should be

propagated to the structural design to benefit a lighter weight structure.

It should be noted that by itself the CDF of the redesign function has little physical significance. Rather, when compared against the CDFs of other structural designs can one get an indication of how invariant a design is to load uncertainty. Future research will seek to provide a comparison of all of the 145 structural designs of the DOE table.

The above represents preliminary results with a main emphasis on the introduction of the noise mode concept. Final results will include probabilistic analysis of each of the structural designs of the DOE table with inclusion of uncertainties for all of the control surfaces and angle of attack and for all four maneuvers to which the structure was designed.

Conclusion

A multidisciplinary design study for AAW technology considering the uncertainty in maneuver loads estimated by linear aerodynamic theory has been presented. The research expands upon the work of Reference [15] by augmenting the rigid aerodynamic force coefficient vectors with uncertainty models based on nonlinear aerodynamics. The study employed design of experiments/response surface methodology and modal-based structural optimization to build deterministic relationships between key structural parameters, such as wing weight, and the gear ratios. Maneuver load uncertainty, associated with the use of linear aerodynamic theory, was then modeled in a probabilistic manner, through noise modes, which represent typical differences between rigid aerodynamic forces predicted by nonlinear and linear aerodynamic theory. The modeled uncertainty was then propagated to a response function, evaluated by static aeroelastic analysis, that was a summation of the violated strain constraints. This function was intended to capture the magnitude of redesign as a result of variation in the loads.

The present research represents a first attempt at introducing load uncertainty into the AAW design process. Upon evaluation of CDFs for all of the structural designs generated for the RSE and considering uncertainties in all control surfaces for all four maneuvers, the designer then can perform a trade-off between weight, performance, and robustness, to determine what value of gear ratios produce the best structural design(s). Future research is aimed at accomplishing this.

Acknowledgements

References

1) Love, M.H., "Integrated Airframe Design at Lockheed Martin Tactical Aircraft Systems," Integrated Airframe Technology, 82nd Meeting of AGARD Structures and Materials Panel, May 1996, AGARD Report 814.

2) Hacklinger, M., "The Development of Manoeuvre Load Criteria for Agile Aircraft," AGARD Workshop on Design Loads for Advanced Fighters, 1988, AGARD Report No. 746.

3) Neubauer, M., Gunther, G., Neunaber, R., "Aircraft Loads and Monitoring," Presented at AGARD SMP Lecture Series on "Aging Combat Aircraft Fleets – Long Term Applications," Madrid, Spain, October 7-8, 1996, AGARD Lecture Series No. 206.

4) Appa, K., "Maneuver Loads Analysis for Military Aircraft," Flight-Vehicle Materials, Structures, and Dynamics – Assessment and Future Directions, Vol. 1, American Society of Mechanical Engineers, 1994.

5) Watson, G.J., "Eurofighter 2000 Structural Design Criteria and Design Loading Assumptions," Loads and Requirements for Military Aircraft, Presented at 83rd Meeting of the AGARD Structures and Materials Panel, Florence, Italy, September 4-5, 1996, AGARD Report 815.

6) Sims, R., McCrosson, P., Ryan, R., and Rivera, J., "X-29A Aircraft Structural Loads Flight Testing," Presented at 20th Annual Society of Flight Test Engineers Symposium, Reno, NV, September 18-21, 1989.

7) Gibson, D.H., "Evolution of F-16 Loads and Requirements," Loads and Requirements for Military Aircraft, Presented at 83rd Meeting of the AGARD Structures and Materials Panel, Florence, Italy, September 4-5, 1996, AGARD Report 815.

8) Miller, G.D., "Active Flexible Wing (AFW) Technology," Air Force Wright Aeronautical Laboratories, TR-87-3096, February 1988.

9) Pendleton, E., Griffin, K., Kehoe, M., and Perry, B., "A Flight Research Program for Active Aeroelastic Wing Technology," 37th AIAA/ ASME/ ASCE/ AHS/ ASC Structures, Structural Dynamics, and Materials Conference, Salt Lake City, UT, April 15-17, 1996.

10) Miller, G.D., "An Active Flexible Wing Multi-Disciplinary Design Optimization Method," 5th AIAA/ USAF/NASA/ISSMO Symposium on Multidisciplinary Analysis and Optimization, Panama City, FL, September 7-9, 1994, AIAA-94-4412.

11) Volk, J., and Ausman, J., "Integration of a Generic Flight Control System into ASTROS," 36th AIAA/ASME/ASCE/AHS/ASC Structures, Structural Dynamics, and Materials Conference, Salt Lake City, UT, April 15-17, 1996, AIAA-96-1335.

12) Zillmer, S., "Integrated Multidisciplinary Optimization for Active Aeroelastic Wing Design," Air Force Wright Aeronautical Laboratories, WL-TR-97-3087, August 1997.

13) Love, M.H., Barker, D.K., Egle, D.D., Neill, D.J., and Kolonay, R.M., "Enhanced Maneuver Airloads Simulation for the Automated Structural Optimization System – ASTROS," 38th AIAA/ ASME/ ASCE/ AHS/ ASC Structures, Structural Dynamics, and Materials Conference, Kissimmee, FL, April 7-10, 1997.

14) Zink, P.S., Mavris, D.N., and Raveh, D.E., "Maneuver Trim Optimization Techniques for Active Aeroelastic Wings," To appear in 41st AIAA/ ASME/ ASCE/ AHS/ ASC Structures, Structural Dynamics, and Materials Conference, Atlanta, GA, April 3-6, 2000.

15) Zink, P.S., Mavris, D.N., Love, M.H., and Karpel, M., "Robust Design for Aeroelastically Tailored/Active Aeroelastic Wing," 7th AIAA/USAF/NASA/ISSMO Symposium on Multidisciplinary Analysis and Optimization, St. Louis, MO, September 2-4, 1998, AIAA-98-4781.

16) Myers, R.H., and Montgomery, D.C., Response Surface Methodology: Process and Product Optimization using Designed Experiments, John Wiley & Sons, Inc., New York, 1995.

17) DeLaurentis, D., Mavris, D.N., and Schrage, D.P., "System Synthesis in Preliminary Aircraft Design using Statistical Methods," 20th Congress of the International Council of the Aeronautical Sciences, Sorrento, Italy, September 1996.

18) Karpel, M., Moulin, B., and Love, M.H., "Modal-Based Structural Optimization with Static Aeroelastic and Stress Constraints," Journal of Aircraft, Vol. 34, No. 3, 1997, pp.433-440.

19) Karpel, M., Moulin, B., and Love, M.H., "Structural Optimization with Stress and Aeroelastic Constraints Using Expandable Modal Basis," 39th AIAA/ASME/ASCE/AHS/ASC Structures, Structural Dynamics, and Materials Conference, Long Beach, CA, 1998.

20) Wu, Y.-T., Millwater, H.R., and Cruse, T.A., "Advanced Probabilistic Structural Analysis Method for Implicit Performance Function," AIAA Journal, Vol. 28, No. 9, 1990, pp. 1663-1669.

21) Southwest Research Institute, FPI User's Manual and Theoretical Manual, San Antonio, TX, 1995.

22) Raveh, D.E., Karpel, M., and Yaniv, S., "Non-Linear Design Loads for Maneuvering Elastic Aircraft," 38th Israel Annual Conference on Aerospace Sciences, Haifa, Israel, February 1998, pp. 150-160 (to appear in Journal of Aircraft).

23) Raveh, D.E., and Karpel, M., "Structural Optimization of Flight Vehicles with Computational-Fluid-Dynamics-Based Maneuver Loads," Journal of Aircraft, Vol. 36, No. 6, 1999, pp. 1007-1015.

24) Rodden, W.P., and Love, J.R., "Equations of Motion of Quasisteady Flight Vehicle Utilizing Restrained Static Aeroelastic Characteristics," Journal of Aircraft, Vol. 22, No. 9, September 1995, pp. 802–809.

25) Johnson, E.H., and Venkayya, V.B., ASTROS Theoretical Manual, AFWAL-TR-88-3028, December 1988.

26) McKay, M.D., Beckman, R.J., and Conover, W.J., "A Comparison of Three Methods for Selecting Values of Input Variables in the Analysis of Output from a Computer Code," Technometrics, Vol. 21, No. 2, May 1979, pp. 239-245.

27) Neill, D.J., Johnson, E.H., and Canfield, R., "ASTROS-A Multidisciplinary Automated Design Tool," Journal of Aircraft, Vol. 27, No. 12, 1990, pp. 1021-1027.

28) Barker, D.K. and Love, M.H., "An ASTROS Application with Path Dependent Results," AIAA/USAF/NASA/ISSMO Multidisciplinary Analysis and Optimization Conference, Bellevue, WA, September 1996.

29) Carmichael, R.L., Castellano, C.R., and Chen, C.F., The Use of Finite Element Methods for Predicting the Aerodynamics of Wing-Body Combinations, NASA SP-228, October 1969.

30) Krist, S.L., Biedron, R.T., and Rumsey, C.L., CFL3D User's Manual Version 5.0, NASA/TM-1998-208444, June 1998

31) Raveh, D.E., Integrated Aero-Structural Design of Maneuvering Flexible Flight Vehicles, Ph.D. Thesis, Technion-Israel Institute of Technology, Haifa, Israel, February 1999.

32) SAS Institute Inc., JMP Computer Program and User's Manual, Cary, NC, 1994.